

Research Article**Atomistic Model Approach to Identify Defects, Lithium Ion Diffusion and Trivalent Dopants in Li_2MnO_2**

^{1,2}Navaratnarajah Kuganathan *, ³Sashikesh Ganeshalingam, ³Poobalasingam Abiman and ^{1,2}Alexander Chroneos

¹Department of Materials, Imperial College London, United Kingdom.

²Faculty of Engineering, Environment and Computing, Coventry University, United Kingdom

³Department of Chemistry, University of Jaffna, Sri Lanka.

Received: 15 March 2018, Accepted: 16 December 2018

Abstract:

Layered lithium-rich metal oxides have attracted great interest as potential cathode materials for Li ion batteries due to their high Li content required for high energy density. Using atomistic simulation techniques based on classical pair potentials, we calculate intrinsic defects, lithium ion diffusion paths together with activation energies and trivalent doping in Li_2MnO_2 . The most favourable intrinsic defect type is found to be the cation anti-site defect, in which Li and Mn ions exchange their positions. Lithium ions diffuse via a zig-zag path with very low activation energy of 0.16 eV. Trivalent dopant Sc^{3+} on Mn site is energetically favourable and could be a synthesis strategy to increase the Li vacancy concentration in Li_2MnO_2 .

Keywords: Defects, Diffusion, Dopants, Atomistic simulation

1. Introduction

The interest in solid-state lithium batteries is driven by the increasing requirement for better capacity, cycle performance, safety, and durability. This motivates the research interest

on the discovery and application of advanced electrolyte and cathode materials (Tarascon & Armand, 2001; Bruce *et al.*, 2011; Jay *et al.*, 2015; Fisher *et al.*, 2013; He *et al.*, 2017; Armstrong *et al.*, 2011; Kuganathan & Islam, 2009; Islam & Fisher, 2014; Kordatos *et al.*, 2018; Kuganathan *et al.*, 2018a; Kuganathan *et al.*, 2018b; Kuganathan *et al.*, 2018c; Kuganathan *et al.*, 2018d; Kuganathan *et al.*, 2018e).

A key area is the identification and study of alternative cathode materials for rechargeable Li-ion batteries. These cathode materials are required to have high energy density to replace more conventional materials and to be employed in large scale applications (i.e. electric vehicles) (Mizushima *et al.*, 1980). In that respect layered Li-rich metal oxides such as Li_2MnO_2 (David *et al.*, 1983; Johnson *et al.*, 2002; Johnson *et al.*, 2003) are of interest as cathode material for Li ion batteries because they have a high Li concentration, which is a prerequisite for the high energy density.

An efficient way to consider the different candidate materials for energy applications is the use of atomic scale modeling techniques. These can provide information on the defect

Corresponding author: Dr. Navaratnarajah Kuganathan, Department of Materials, Imperial College London, London, SW7 2AZ, United Kingdom and Faculty of Engineering, Environment and Computing, Coventry University, Priory Street, Coventry CV1 5FB, United Kingdom. e-mail: ad0636@coventry.ac.uk



This article is published under the Creative Commons (CC BY-NC-ND) License (<http://creativecommons.org/licenses/by-nd/4.0/>).

This license permits use, distribution and reproduction, non-commercial, provided that the original work is properly cited and is not changed in anyway.

processes including Li ion energetics and mechanisms that can be complementary to experimental work. There is no related theoretical work on the Li related defect process in Li_2MnO_2 . The present investigation employs established atomistic modeling techniques based on classical pair potentials to study the intrinsic defect processes, lithium ion diffusion mechanisms and the impact of trivalent doping (Al, Sc, In, Y, Gd and La) in Li_2MnO_2 .

2. Computational Methods

All calculations were carried out using the classical pair potential method as implemented in the GULP package (Gale & Rohl, 2003). This method is based on the classical Born model description of an ionic crystal lattice. All systems were treated as crystalline solids with interactions between ions consisting of long-range attractions and short-range repulsive forces representing

electron-electron repulsion and van der Waals interactions. The short range interactions were modelled using Buckingham potentials available in the literature (Table 1). Simulation boxes and the corresponding atom positions were relaxed using the Broyden-Fletcher-Goldfarb-Shanno (BFGS) algorithm (Gale, 1997). The Mott-Littleton method (Mott & Littleton, 1938) was used to investigate the lattice relaxation about point defects and the migrating ions. It divides the crystal lattice into two concentric spherical regions, where the ions within the inner spherical region (on the order of >700 ions) immediately surrounding the defect relaxed explicitly. Li ion diffusion was calculated considering two adjacent vacancy sites as initial and final configurations. Seven interstitial Li ions were considered in a direct linear route and they were fixed while all other ions were free to relax. The local maximum energy along this diffusion path is calculated and reported as activation energy.

Table 1: Buckingham interatomic potential parameters {Two-body [$\Phi_{ij}(r_{ij}) = A_{ij} \exp(-r_{ij}/\rho_{ij}) - C_{ij}/r_{ij}^6$]} used in the atomistic simulations of Li_2MnO_2 (Kuganathan & Islam, 2009; Islam et al., 2005; Minervini et al., 1999).

Interaction	A (eV)	ρ (Å)	C (eV·Å ⁶)	Y (e)	K (eV·Å ⁻²)
Li ⁺ - O ²⁻	632.1018	0.2906	0.000	1.000	99999
Mn ²⁺ - O ²⁻	2601.394	0.2780	0.000	3.420	95.0
O ²⁻ - O ²⁻	22764.30	0.1490	27.89	-2.860	74.92
Al ³⁺ - O ²⁻	1725.20	0.28971	0.000	3.000	99999
Sc ³⁺ - O ²⁻	1575.85	0.3211	0.000	3.000	99999
In ³⁺ - O ²⁻	1495.65	0.3327	4.33	3.000	99999
Y ³⁺ - O ²⁻	1766.40	0.33849	19.43	3.000	99999
Gd ³⁺ - O ²⁻	1885.75	0.3399	20.34	3.000	99999
La ³⁺ - O ²⁻	2088.79	0.3460	23.25	3.000	99999

3. Results and Discussion

3.1. Structural Modelling

The starting point of this study was to test the quality of the interatomic potentials used in this study by performing a total energy calculation of the Li_2MnO_2 crystal. The layered structure of Li_2MnO_2 (David et al., 1983)

exhibits a hexagonal type lattice (space group: $P\bar{3}m1$) as shown in *Figure 1*.

Energy minimization calculations were performed on Li_2MnO_2 structure to obtain the equilibrium lattice constants. The calculated equilibrium lattice constants (refer Table 2) are in good agreement with experiment.

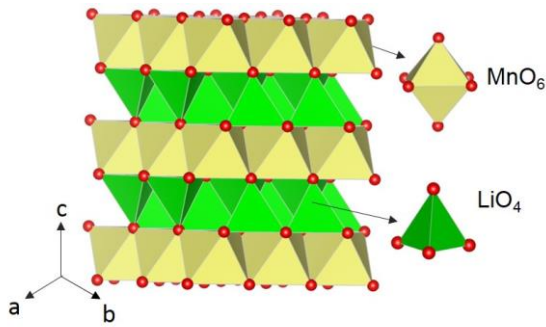


Figure 1: Crystal structure of layered Li_2MnO_2 (David et al., 1983). Manganese and lithium atoms form octahedron and tetrahedron respectively with adjacent oxygen atoms

Table 2: Calculated and experimental (David et al., 1983) structural parameters for layered hexagonal ($P\bar{3}m1$) Li_2MnO_2

Parameter	Calculated	Experimental	$ \Delta (\%)$
a (Å)	3.1950	3.1571	1.18
b (Å)	3.1950	3.1571	1.18
c (Å)	5.3030	5.1964	2.01
$\alpha = \beta$	90.00	90.00	0.00
γ (°)	120.0	120.0	0.00

3.2. Intrinsic Defects

To calculate the formation energies for Frenkel and Schottky-type defects in Li_2MnO_2 , a series of isolated point defect (vacancy and interstitial) energies were calculated. The equations represent the reactions involving these defects as written using Kröger-Vink notation (Kröger & Vink, 1956) and corresponding reaction energies are tabulated in Table 3.

It is calculated that the most favorable intrinsic disorder is the Li-Mn anti-site defect (equation 8). In this defect, Li^+ and Mn^{2+} ions interchange their positions. The exact concentration of this defect is dependent on the temperature and synthesis routes. The formation of Li Frenkel is the second most favorable defect process in this material. As Mn Frenkel, O Frenkel and Schottky defects are highly energetically unfavorable and thus it is unlikely to occur in any significant concentration in Li_2MnO_2 .

Table 3: Energetics of intrinsic defects in Li_2MnO_2 .

Defect Process	Equation	Defect energy (eV)	Defect energy (eV)/defect
Li Frenkel/1	$\text{Li}_{\text{Li}}^{\text{X}} \rightarrow V'_{\text{Li}} + \text{Li}_i^{\bullet}$	2.59	1.30
O Frenkel/2	$\text{O}_{\text{O}}^{\text{X}} \rightarrow V_{\text{O}}^{\bullet\bullet} + \text{O}_i''$	9.50	4.75
Mn Frenkel/3	$\text{Mn}_{\text{Mn}}^{\text{X}} \rightarrow V''_{\text{Mn}} + \text{Mn}_i^{\bullet\bullet}$	5.29	2.65
Schottky/4	$2 \text{Li}_{\text{Li}}^{\text{X}} + \text{Mn}_{\text{Mn}}^{\text{X}} + 2 \text{O}_{\text{O}}^{\text{X}} \rightarrow 2 V'_{\text{Li}} + V''_{\text{Mn}} + 2 V_{\text{O}}^{\bullet\bullet} + \text{Li}_2\text{MnO}_2$	12.97	2.59
Li_2O Schottky-like/5	$2 \text{Li}_{\text{Li}}^{\text{X}} + \text{O}_{\text{O}}^{\text{X}} \rightarrow 2V'_{\text{Li}} + V_{\text{O}}^{\bullet\bullet} + \text{Li}_2\text{O}$	5.84	1.94
MnO Schottky-like/6	$\text{Mn}_{\text{Mn}}^{\text{X}} + \text{O}_{\text{O}}^{\text{X}} \rightarrow V''_{\text{Mn}} + V_{\text{O}}^{\bullet\bullet} + \text{MnO}$	7.02	3.51
Li/Mn anti-site (isolated)/7	$\text{Li}_{\text{Li}}^{\text{X}} + \text{Mn}_{\text{Mn}}^{\text{X}} \rightarrow \text{Li}'_{\text{Mn}} + \text{Mn}_{\text{Li}}^{\bullet}$	2.90	1.45
Li/Mn anti-site (cluster)/8	$\text{Li}_{\text{Li}}^{\text{X}} + \text{Mn}_{\text{Mn}}^{\text{X}} \rightarrow \{\text{Li}'_{\text{Mn}}: \text{Mn}_{\text{Li}}^{\bullet}\}^{\text{X}}$	2.00	1.00

3.3. Li ion Diffusion

The intrinsic lithium ion diffusion in and out of the Li_2MnO_2 material determines its use as a possible high-rate cathode material in lithium batteries. The diffusion paths in the Li_2MnO_2 material have not been established experimentally. Using atomistic simulation techniques it is possible to examine various possible diffusion paths responsible for lithium ion diffusion. Two main long range diffusion channels (A and B) connecting local

Li hops (see Figure 2(a)) have been identified. The lowest activation energy is calculated to be 0.16 eV for the channel A. Channel A forms a zig-zag pattern with equal Li-Li separation of 2.24 Å. Channel B is slightly different and it exhibits a straight line path with the higher activation energy. Individual Li-Li separations and corresponding activation energy barriers are tabulated in Table 4. Potential energy profile diagram for the Li hopping in channel A is shown in Figure 2(b).

Table 4: Calculated Li-Li separations and activation energies for the lithium ion migration between two adjacent Li sites as shown in Figure 2a

Migration path	Li-Li separation (Å)	Activation energy (E_a)(eV)
A	2.24	0.16
B	3.16	2.38

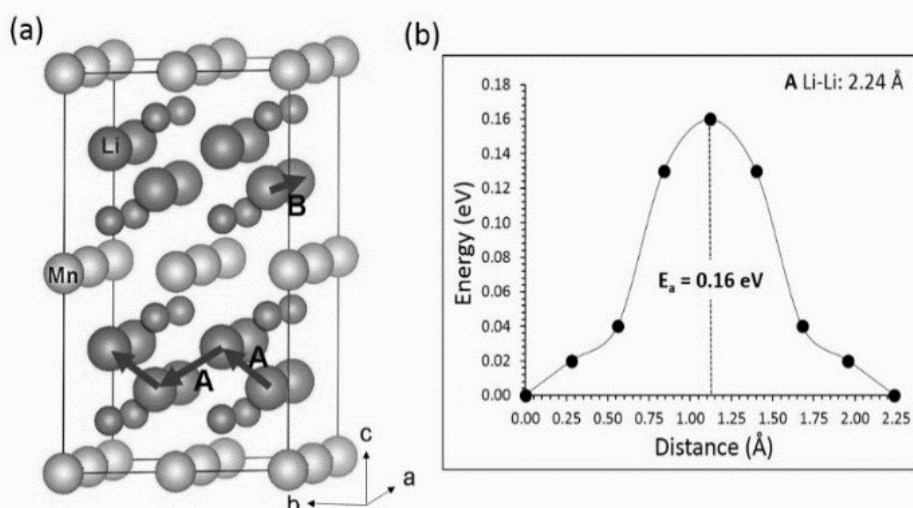
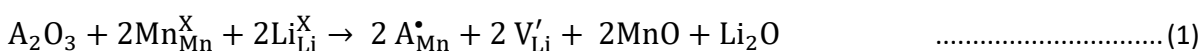


Figure 2: (a) Lithium vacancy migration paths considered
(b) Energy profile diagram of Li vacancy hopping between two adjacent Li sites in channel A

3.4. Trivalent Doping

In previous sections, we have shown that Li ions can diffuse with lower activation energy of 0.16 eV. However, the concentration of Li ions in the lattice is dependent on the Li Frenkel

energy (1.30 eV/defect) which limits the concentration of V'_{Li} . Here we suggest a way to increase the concentration by substituting trivalent dopants (A) on Mn site (A=Al, Sc, In, Y, Gd and La). This processes can be described as (using the Kröger-Vink notation):



Calculated solution energies together with the ionic radii of trivalent dopants are shown in Figure 3. The lowest solution energy is calculated for Sc^{3+} . This means that the Sc^{3+} is the candidate trivalent dopant that can enhance the concentration of Li vacancy defects in Li_2MnO_2 . The second lowest solution energy is calculated for In^{3+} with the energy difference of 0.40 eV compared to that of Sc^{3+} . Other dopants exhibit high positive solution energies meaning that they are less likely to enhance Li vacancy concentration at low temperature.

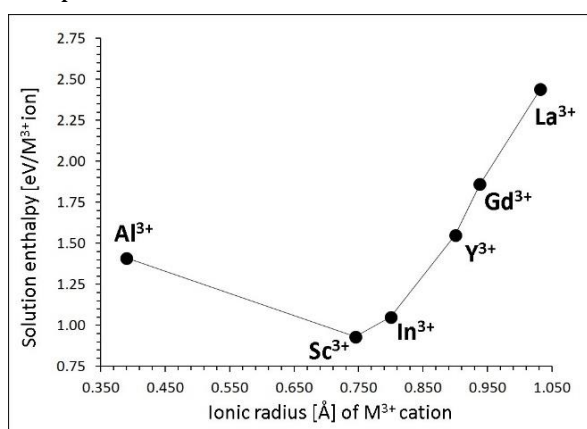


Figure 3: Enthalpy of solution of A_2O_3 ($\text{A} = \text{Al}, \text{Sc}, \text{In}, \text{Y}, \text{Gd}$ and La) in Li_2MnO_2

4. Conclusions

Atomistic modelling techniques have been employed to investigate the key issues related to point defects, lithium ion diffusion and dopants in the Li_2MnO_2 material. Our simulation shows good reproduction of the experimental crystal structure of Li_2MnO_2 . The most favourable intrinsic disorder type is the Li-Mn anti-site defect. A long range zig-zag Li ion diffusion path with a very low activation energy (0.16 eV) was found. This clearly shows that Li can easily diffuse once the Li vacancies are available. In order to increase the Li vacancies, trivalent dopants were considered. The most energetically favourable dopant on the Mn site is Sc^{3+} .

5. Acknowledgement

Computational facilities and support were provided by High Performance Computing Centre at Imperial College London and the Department of Chemistry, University of Jaffna. Prof. Julian Gale (Faculty of Science and Engineering, Curtin University, Australia) is acknowledged for allowing the members of the department to download and run GULP code on their personal computers.

References

- Armstrong, A.R., Kuganathan, N., Islam, M.S. & Bruce, P.G. (2011). Structure and Structure and Lithium Transport Pathways in $\text{Li}_2\text{FeSiO}_4$ Cathodes for Lithium Batteries. *Journal of the American Chemical Society*, 133(33), 13031-13035. Retrieved from <https://doi.org/10.1021/ja2018543>
- Bruce, P.G., Freunberger, S.A., Hardwick, L.J. & Tarascon, J.M. (2011). Li-O₂ and Li-S Batteries with High Energy Storage. *Nature Materials*, 11(1), 19-29. doi:10.1038/nmat3191
- David, W. I. F., Goodenough, J. B., Thackeray, M. M. & Thomas, M. G. S. R. (1983). The Crystal structure of Li_2MnO_2 . *Revue de Chimie Minerale*, 20(4-5), 636-642.
- Fisher, C.A.J., Kuganathan, N. & Islam, M.S. (2013). Defect chemistry and lithium-ion migration in polymorphs of the cathode material $\text{Li}_2\text{MnSiO}_4$. *Journal of Materials Chemistry A*, 1(13), 4207-4214. doi:10.1039/C3TA00111C
- Gale, J.D. & Rohl, A.L. (2003). The General Utility Lattice Program (GULP). *Molecular Simulation*, 29(5), 291-341. doi:<https://doi.org/10.1080/0892702031000104887>
- Gale, J.D. (1997). GULP: A computer program for the symmetry-adapted simulation of solids. *Journal of the Chemical Society, Faraday Transactions*, 93(4), 629-637.
- He, X., Zhu, Y. & Mo, Y. (2017). Origin of fast ion diffusion in super-ionic conductors. *Nature Communications*, 8, 15893.

- Islam, M.S. & Fisher, C.A.J. (2014). Lithium and sodium battery cathode materials: computational insights into voltage, diffusion and nanostructural properties. *Chemical Society Reviews*, 43 (1), 185-204. doi:10.1039/C3CS60199D
- Islam, M.S., Driscoll, D.J., Fisher, C.A.J. & Slater, P.R. (2005). Atomic-Scale Investigation of Defects, Dopants, and Lithium Transport in the LiFePO₄ Olivine-Type Battery Material. *Chemistry of Materials*, 17(20), 5085-5092. doi:10.1021/cm050999v
- Jay, E.E., Rushton, M.J.D., Chroneos, A., Grimes, R.W. & Kilner, J.A. (2015). Genetics of superionic conductivity in lithium lanthanum titanates. *Physical Chemistry Chemical Physics*, 17(1), 178-183.
- Johnson, C.S., Kim, J-S., Kropf, A.J., Kahaian, A.J., Vaughey, J.T. & Thackeray, M.M. (2002). The role of Li₂MO₂ structures (M=metal ion) in the electrochemistry of (x)Li₂Mn_{0.5}Ni_{0.5}O₂(1-x)Li₂TiO₃ electrodes for lithium-ion batteries. *Electrochemistry Communications*, 4(6), 492-498. Retrieved from [https://doi.org/10.1016/S1388-2481\(02\)00346-6](https://doi.org/10.1016/S1388-2481(02)00346-6)
- Johnson, C.S., Kim, J-S., Kropf, A.J., Kahaian, A.J., Vaughey, J.T., Fransson, L. M. L., Edström, K. & Thackeray, M.M. (2003). Structural Characterization of Layered Li_xNi_{0.5}Mn_{0.5}O₂ (0 < x ≤ 2) Oxide Electrodes for Li Batteries. *Chemistry of Materials*, 15(12), 2313-2322. Retrieved from <https://doi.org/10.1021/cm0204728>
- Kordatos, A., Kuganathan, N., Kelaidis, N., Iyngaran, P. & Chroneos, A. (2018). Defects and lithium migration in Li₂CuO₂. *Scientific Reports*, 8(1), 6754. doi:10.1038/s41598-018-25239-5
- Kröger, F.A. & Vink, H.J. (1956). Relations between the Concentrations of Imperfections in Crystalline Solids. In F. Seitz, & D. Turnbull (Eds.), *Solid State Physics* (Vol. 3, pp. 307-435). Massachusetts: Academic Press. Retrieved from [https://doi.org/10.1016/S0081-1947\(08\)60135-6](https://doi.org/10.1016/S0081-1947(08)60135-6)
- Kuganathan, N. & Chroneos, A. (2018a). Defects, Dopants and Sodium Mobility in Na₂MnSiO₄. *Scientific Reports*, 8, 14669. doi:10.1038/s41598-018-32856-7
- Kuganathan, N. & Islam, M.S. (2009). Li₂MnSiO₄ Lithium Battery Material: Atomic-Scale Study of Defects, Lithium Mobility, and Trivalent Dopants. *Chemistry of Materials*, 21(21), 5196-5202. Retrieved from <https://doi.org/10.1021/cm902163k>
- Kuganathan, N., Ganeshalingam, S. & Chroneos, A. (2018b). Defects, Dopants and Lithium Mobility in Li₉V₃(P₂O₇)₃(PO₄)₂. *Scientific Reports*, 8, 8140. doi: 10.1038/s41598-018-26597-w
- Kuganathan, N., Iyngaran, P. & Chroneos, A. (2018c). Lithium diffusion in Li₅FeO₄. *Scientific Reports*, 8, 5832. doi:10.1038/s41598-018-24168-7
- Kuganathan, N., Kordatos, A. & Chroneos, A. (2018d). Li₂SnO₃ as a Cathode Material for Lithium-ion Batteries: Defects, Lithium Ion Diffusion and Dopants. *Scientific Reports*, 8, 12621.
- Kuganathan, N., Kordatos, A., Fitzpatrick, M.E., Vovk, R.V. & Chroneos, A. (2018e). Defect process and lithium diffusion in Li₂TiO₃. *Solid State Ionics*, 327, 93-98. doi:<https://doi.org/10.1016/j.ssi.2018.10.030>
- Minervini, L. Z. (1999). Defect cluster formation in M₂O₃-doped CeO₂. *Solid State Ionics*, 116(3-4), 339-349.
- Mizushima, K. J. (1980). Li_xCOO₂ (0<x<-1): A new cathode material for batteries of high energy density. *Materials Research Bulletin*, 15(6), 783-789.
- Mott, N. F. (1938). Conduction in polar crystals. I. Electrolytic conduction in solid salts. *Transactions of the Faraday Society*, 34, 485-499. doi:10.1039/TF9383400485
- Tarascon, J. & (2001). Issues and challenges facing rechargeable lithium batteries. *Nature*, 414, 359-367.